High-pressure experimental and theoretical investigations on the fluorite structured compound $AuAl_2$

Alka B. Garg, Ashok K. Verma, V. Vijayakumar, R. S. Rao, and B. K. Godwal
High Pressure Physics Division, Purnima Laboratories, Bhabha Atomic Research Centre, Mumbai 400085, India
(Received 3 February 2005; published 20 July 2005)

Diamond anvil cell (DAC) based resistance measurements are carried out in $AuAl_2$ to the pressures of about 25 GPa for the first time. The data indicate possibility of phase transition around 12 GPa. High pressure data obtained using Elettra synchrotron source confirm the transformation of $AuAl_2$ from ambient CaF_2 to orthorhombic phase. The high precision *P-V* data when transformed to universal equation of state does not show any deviation from linearity. The first principles electronic band structure calculations up to these pressures in the cubic phase do not reveal any change corroborating the experimental findings of nonobservation of electronic topological transition in this compound.

DOI: 10.1103/PhysRevB.72.024112 PACS number(s): 61.10.Nz, 05.70.Fh, 71.20.Ps, 07.35.+k

INTRODUCTION

The intermetallics, with CaF_2 structure [Space Group (SG) $Fm3m$] are of significant interest due to their interesting properties.[1] Most of the materials having fluorite structure are halides, oxides, or chalcogenides of univalent or tetravalent cations and show predominantly ionic bonding. However, the intermetallics of gold and platinum (A) with Al, Ga, and In (X) are the few that crystallize in the CaF_2 structure.[2] While the fluorite structure is the stable form at room temperature for all the Au compounds and $PtAl_2$, it is stable at high temperatures only for $PtGa_2$ and $PtIn_2$.[3] These phases exhibit a striking variety of colors ranging from violet ($AuAl_2$) to copper ($PtIn_2$) to brass ($PtAl_2$, $PtGa_2$).[4] In them, the A-X distance is about 0.2 Å less than the sum of the 12 coordination radii of the constituent atoms suggesting a covalent character of the bond. These compounds also serve as prototype materials for studying the Au/Pt (A) $5d$ bands in intermetallics at larger A-A separation. The primitive cell contains one A atom and two X atoms with seven valence electrons (one from Au/Pt and three from each X atom). This leads to good electric conductivity resulting in applications of $AuAl_2$ as a spectral selective solar absorber[5] and of $PtAl_2$ as a corrosion resistant metallic material.[6] Low temperature studies in these compounds show that many of them become superconducting with low T_c and are employed in reference devices for precision thermometry below 1 K.[7]

The electronic structure of AX_2 intermetallics has been investigated by both computationally[8] and experimentally.[9–13] X-ray absorption near edge spectroscopy measurements on $AuAl_2$ shows that there is a strong chemical bonding with a depletion of the effective $5d$ orbital count.[14] The substantial chemical bonding involving the Au-$5d$ orbital in the $AuAl_2$, is evidenced by strong enhancement of $2p \rightarrow 5d$ (L_2 and L_3 edges) transitions. In $AuAl_2$ the hole count change induced by chemical bonding is distributed between $5d^{5/2}$ and $5d^{3/2}$ states and is the cause of violet color of $AuAl_2$.[14]

In AuX_2 compounds the lattice constants increases monotonically with temperature from 4.2 K to room temperature for $AuAl_2$ and $AuIn_2$ and to 715 K for $AuGa_2$ (Ref. 15) with observation of volume contraction in all these materials on melting.[3] Earlier investigations on the variation of melting point with pressure on[3] AuX_2 (X=In, Ga, and Al) reveal that it decreases with pressure for $AuGa_2$ and $AuAl_2$, while for $AuIn_2$ it remains constant to about 3 GPa and then acquires a positive slope at higher pressures nearing 5 GPa.

The earlier studies on $AuIn_2$ (Ref. 12) at ambient temperature on variation of resistance and thermoelectric power (TEP) with pressure indicated presence of electronic or structural change around the pressure anomaly in the fusion data of storm *et al.*[3] Synchrotron based high pressure angle dispersive x-ray diffraction (ADXRD) measurements ruled out the structural transition at the anomaly. However the high precision *P-V* data at the close intervals when transformed to universal equation of state (UEOS) showed deviation from linearity around the anomaly. The first principle band structure calculations with pressure revealed the electronic topologic transition (ETT)[16] as the cause of anomaly. $AuIn_2$ was also found to undergo structural transition beyond 9 GPa.[13] In contrast to this $AuAl_2$ does not show any anomaly in the fusion data. As the fusion anomaly under compression in $AuIn_2$, the peak in pressure variation of TEP and deviation from linearity in UEOS are correlated to the occurrence of ETT then the above features should not be seen in the $AuAl_2$. In order to confirm this and firmly associate the ETT to the anomaly in fusion data and UEOS we have carried out the high pressure transport, ADXRD and theoretical electronic band structure studies on $AuAl_2$ to look for absence of anomalies in transport and UEOS at lower pressure and also to investigate the possibility of structural phase transition in it like the intermetallic $AuIn_2$.

EXPERIMENT

Sample preparation

$AuAl_2$ was prepared by arc melting appropriate amounts of the components under argon atmosphere followed by annealing for one week. The sample was characterized for purity by chemical analysis and XRD. The measured lattice parameter 6.0049 Å is in good agreement with the literature value.[17]

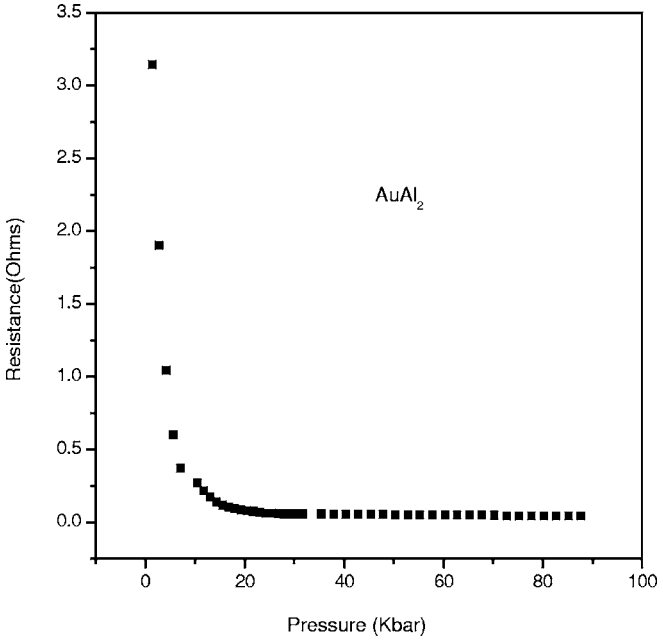

FIG. 1. Pressure variation of electrical resistance for $AuAl_2$ up to 9 GPa.

Electrical resistance measurements

For electrical resistance measurements up to 9 GPa, an opposed Bridgman anvil apparatus was used, as it gives better resolution in lower pressure region (as compared to DAC measurements). Pyrophyllite gaskets for pressure containment, and steatite (talc) for pressure transmission, were employed. The electrical resistance measurements under pressure were carried out by the four probe techniques with *in-situ* Bi calibration. For four probe measurements, stainless steel lead wires of 40 μm diameter are employed. Details of the technique are given elsewhere.[18] Thin sheets of the materials of approximate size 3 mm $\times$ 5 mm with a thickness of 0.2 mm were prepared, and then pressed between tungsten carbide anvils to a load of 5 tons. The flattened material was then trimmed to pieces of 1.5 mm long and 2.5 mm wide pieces and used for the measurements.

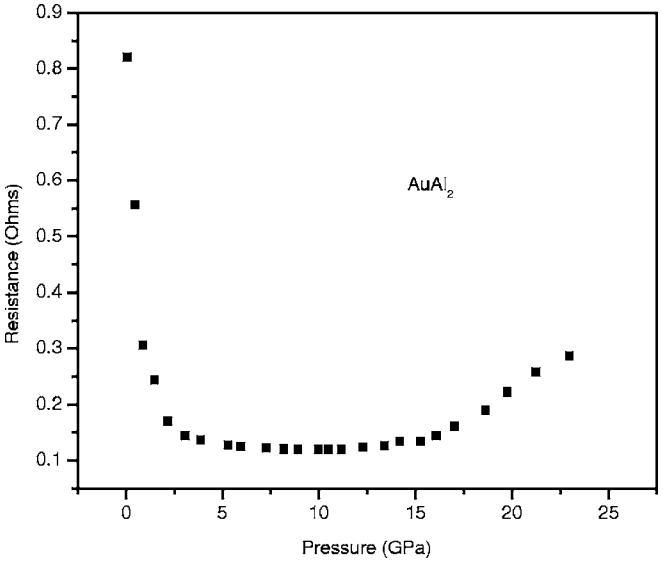

FIG. 2. Pressure variation of electrical resistance for $AuAl_2$ up to 25 GPa.

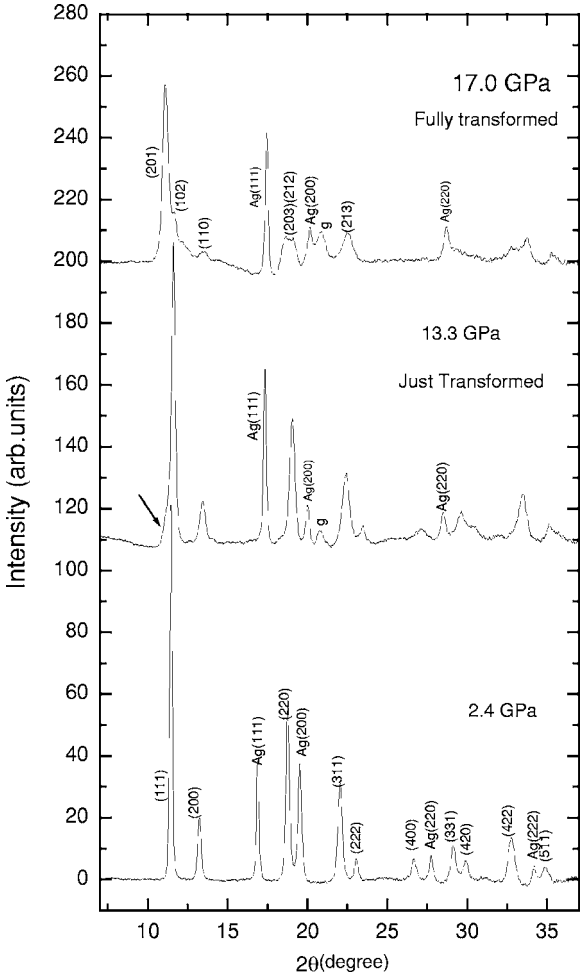

FIG. 3. Pressure evolution of diffraction patterns for $AuAl_2$.

To extend the measurements to higher pressure region, our recently commissioned diamond anvil cell (DAC) based technique was used.[19] A clamp type Merrill Bessett DAC with a diamond culet size of 400 μm and stainless steel gasket was employed. Myler embedded alumina was used as a pressure transmitting medium. 20 μm diameter stainless steel wires, at a separation of $\sim$30 μm or less are used as leads for quasi-four probe measurements. Pressure was measured by ruby fluorescence technique. A small rectangular piece of the sample prepared by pressing it between the two diamonds of another cell (thickness $\sim$5 μm) was kept at the center of the anvil face touching both wires. Constant current is passed through the two leads and voltage is measured across the sample. The pressure variation of electrical resistance of $AuAl_2$ up to 9 GPa is shown in Fig. 1. The resistance decreases continuously up to 9 GPa. This is consistent with the absence of any slope change in the fusion behavior[3] and indicates the absence of any structural or isostructural transition until 9 GPa. The results of DAC based resistance measurements up to 25 GPa is shown in Fig. 2. The decrease in electrical resistance continues up to 12 GPa indicating the

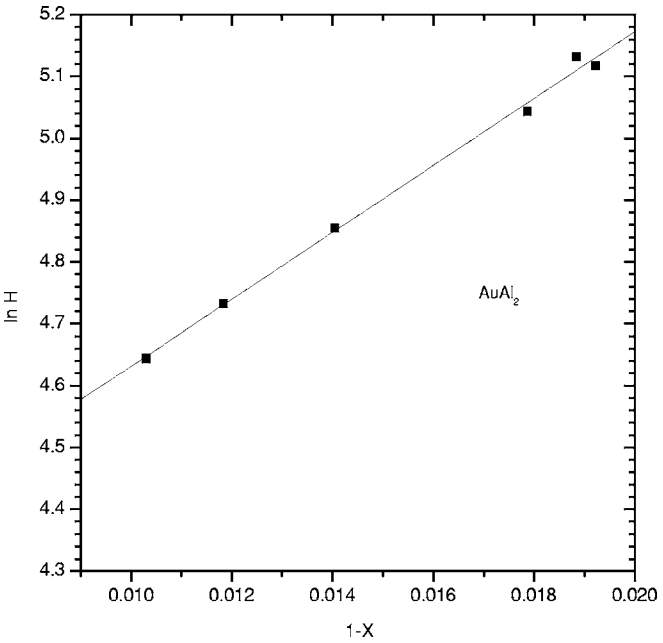

FIG. 4. Measured universal equation of state for $AuAl_2$.

absence of ETT in this pressure region. However above 12.5 GPa, the resistance starts increasing slowly and beyond 16 GPa it increases faster. This indicates the presence of structural phase transition above 12 GPa.

ADXRD measurements

In order to correlate the results of electrical resistance measurements to a structural phase transition, high pressure ADXRD measurements were carried out at the x-ray diffraction beam line of Elettra synchrotron source, Italy under proposal No. 1999389. A modified Mao-Bell[20] type diamond anvil was used for pressure generation. Powdered sample along with silver as pressure calibrant, and ethanol as pressure transmitting medium, was loaded inside a hardened stainless steel preindented gasket hole of diameter 100 μm. The two-dimensional (2D) diffraction images recorded on a Mar research image plate detector were collapsed to one-dimensional (1D) diffraction patterns using FIT2D software.[21] Sample to film distance was calibrated by taking palladium powder pattern as standard. X-ray powder patterns at various pressures from $AuAl_2$ were collected employing x rays of wavelength 0.687 96 Å (calibrated) at various pressures. The evolution of X-ray diffraction patterns is shown in Fig. 3. The diffraction patterns do not show any structural phase transition until 12 GPa. However at 12.3 GPa a small kink is seen in the (111) line and beyond 16 GPa, this line gets split into two lines. Also new diffraction peaks appear indicating the occurrence of a gradual structural phase transition (Fig. 3).

The occurrence of electronic transition may be identified from equation of state (EOS) measurements by converting the *P-V* data to universal equation of state (UEOS). Any deviation from linearity in the UEOS indicates the presence of an electronic transition.[22] The equation of state for cubic phase when converted to universal equation of state does not show any deviation from linearity hence ruling out the possibility of any electronic transition (Fig. 4).

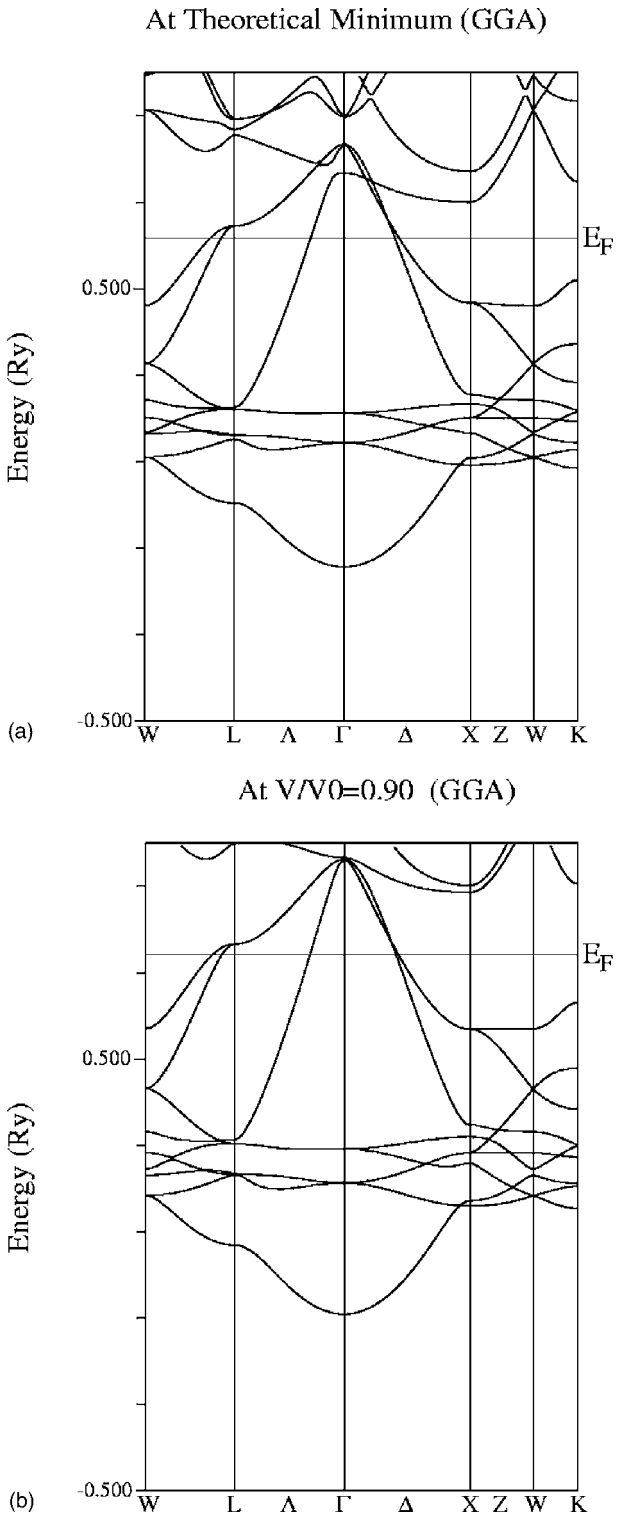

FIG. 5. (a) Theoretical band structure in the Γ-*L* direction at ambient pressure. (b) Theoretical band structure in the Γ-*L* direction at 9 GPa.

BAND STRUCTURE CALCULATIONS

To further strengthen our experimental inference of absence of ETT through UEOS the total energy calculations

TABLE I. Indexing of $AuAl_2$ at 17 GPa to an orthorhombic cell. $A=8.067$ Å, $B=3.177$ Å, $c=7.472$ Å.

d_{obs}	d_{cal}	h	k	l
3.5490	3.5494	2	0	1
3.3888	3.3901	1	0	2
2.9266	2.9241	0	1	1
2.1234	2.1192	2	0	3
2.0671	2.0755	2	1	2
1.7604	1.7631	2	1	3
1.3594	1.3541	5	0	3
1.2144	1.2102	0	2	4

were performed using the full potential linear augmented plane wave method (FP-LAPW), as implemented in the WIEN2K computer program.[23] This is based on density functional theory and is first principle in nature with only atomic number of the elements as input. The errors in this approach are limited to the approximation of the exchange-correlation energy functional, cutoffs in the expansion of the basis functions, **k**-point sampling in the integrations over the Brillouin zone, and Born-Oppenheimer approximation. In the FP-LAPW method there is no approximations as regards the crystal geometry; the charge density and potential can have arbitrary shape though the wave functions are only variational approximations of the true wave functions in the region of fixed energies E_ν. Thus relatively open CaF_2 structure can be tackled without loss of precision. The calculation is fully relativistic for the core states but semirelativistic with variational treatment of spin-orbit coupling for the valence states. For the exchange-correlation terms both the local density approximation (LDA)[24] and the generalized gradient approximation (GGA)[25] were used. Muffin-tin radii (R_{mt}) of two Bohr units were employed for both Au ($5s^25p^64f^{14}5d6s$) and Al ($2s^22p^63s^23p^1$). The desired precision in the total energy is achieved by using a plane wave cutoff $R_{mt}K_{max}=9$ and a **k**-point sampling in the Brillouin zone (BZ) of 2000 points. In order to get the equilibrium volume, the *ab initio* energy-volume data was fitted to a fourth-order polynomial and the equilibrium volume was identified from the minimum of the curve. The computed equilibrium volume is overestimated by 3% in the case of GGA and underestimated by 2% in the case of LDA. These results are within the acceptable error range that generally occurs in the density functional based first principles calculations. The computations were carried out at high pressures to investigate the possibility of a band extremum crossing the Fermi level (electronic topological transition, ETT) under pressure. Figures 5(a) and 5(b) show the band structure of the $AuAl_2$ at the theoretical equilibrium volume and at the $V/V_0=0.9$, respectively. It is clear from these that no ETT occurs up to the pressure corresponding to $V/V_0=0.9$. $AuAl_2$ is stable in the CaF_2 structure in this pressure range as revealed by the ADXRD data. Thus, $AuAl_2$ does not show an ETT under pressure unlike other intermetallics $AuX_2(X=In,Ga)$ which show an ETT under pressure.

The bulk modulus and it's pressure derivative in the CaF_2 phase obtained by fitting the experimental *P-V* data up to 12 GPa to *B-M* EOS are 111 GPa and 4, respectively. The bulk modulus estimated from the computed *P-V* relation is 103 GPa (126 GPa in case of LDA), which are in good agreement with the measured value of 111 GPa. Using these values of bulk modulus and equilbrium volumes, the estimated Debye temperature is 289 K (317 K in LDA) which is in good agreement with the experimental value of 297 K.[26]

The high pressure phase for $AuAl_2$ can be indexed to an orthorhombic cell ($A=8.067$ Å, $B=3.177$ Å, $C=7.472$ Å at 17 GPa, Table I). The pressure volume data up to 17 GPa is shown in Fig. 6. This cell is closely related to the CaF_2 phase ($A_0=\sqrt{2}^*A_c$, $B_0=A_c/2$, and $C_0=\sqrt{2}^*A_c$) consistent with the close similarity of the diffraction pattern to that of the CaF_2 phase. This implies a discontinuous volume change of 3.5% at the transition. The systematic absences implies that the space groups (SGs) may be one among the possible $Pnm2_1(31)$, $Pnmm(59)$, $Pn2_1(33)$, and $Pnma(62)$. Because of the low symmetry of the structure and the few lines available, no attempt was made for a complete structural analysis of the high pressure phase. However, the possibility of the

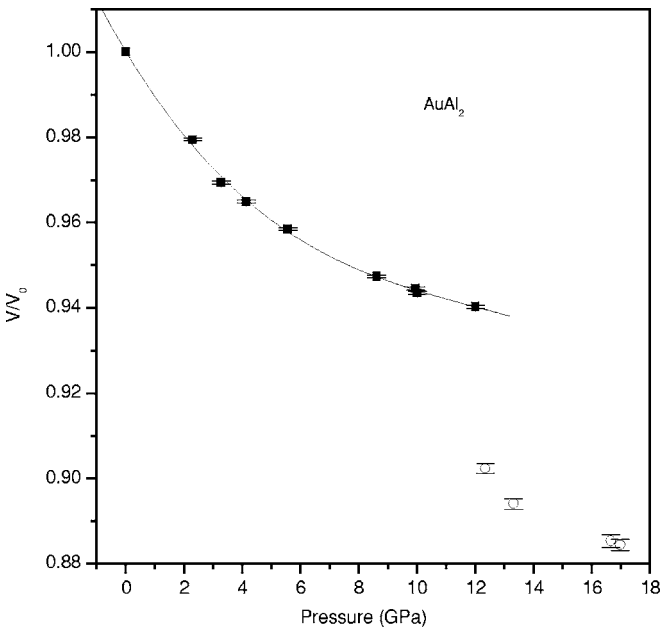

FIG. 6. Experimental EOS for $AuAl_2$.

structure being one among the post CaF_2 structures seen in halides and oxides at high pressures is excluded, as none of them fits the present data.[27] Another interesting aspect of this structural analysis is that the lines are in general broad (although Ag lines are sharp) and also there is an increase in background intensity after the transition. The evolution of the structure, which indicates progressive departure from the CaF_2 structure, and increasing background, is consistent with the increase in electrical resistance with pressure. In view of the indicated disorder of the structure, the possibility of this structure being related to structures separated from CaF_2 structure by entropy barriers was also examined.[28] The structure does not belong to this category also. A detailed investigation of this high pressure phase by EXAF or powder diffraction at the IVth generation synchrotron source is needed.

CONCLUSIONS

Results of x-ray diffraction and transport measurements do not show ETT and is consistent with the high pressure fusion data. The first principles electronic structure theory corroborates these experimental findings. We notice $AuAl_2$ undergoing gradual structural phase transition beyond 12.5 GPa to an orthorhombic phase. The present work thus confirms that the anomalies present in fusion, electrical and UEOS data of $AuIn_2$ and $AuGa_2$ are uniquely correlated to ETT as evidenced by their absence in $AuAl_2$.

ACKNOWLEDGMENT

Two of the authors (A.B.G. and V.V.K.) thankfully acknowledge the ICTP for travel support and hospitality at Elettra.

[1] L. S. Hsu, Mod. Phys. Lett. B **8**, 1297 (1994).
[2] C. Barrett and T. B. Massalski, *Structure of Metals*, McGraw-Hill Series in Material Science and Engineering (McGraw-Hill, Eurasia, New Delhi, 1966).
[3] A. R. Storm, J. H. Wernick, and A. Jayaraman, J. Phys. Chem. Solids **27**, 1227 (1966).
[4] E. Zintl, A. Harder, and W. Haucke, Z. Phys. Chem. Abt. B **B35**, 354 (1937).
[5] E. Hahn and B. O. Seraphin, Phys. Thin Films **10**, 1 (1978).
[6] R. Streiff, J. Mater. Eng. **10**, 15 (1988).
[7] J. H. Wernick, A. Menth, T. H. Geballe, G. Hull, and J. P. Maita, J. Phys. Chem. Solids **30**, 1949 (1969); W. P. Bosch, A. Chinchure, J. Flokstra, M. J. de Groot, E. Van Heumen, R. Jochemsen, F. Mathu, A. Peruzzi, and D. Veldhuis, http://www.xs4all.nl/~hdleiden/srd1000/reports/srd 1000. doc
[8] A. C. Switendick and A. Narath, Phys. Rev. Lett. **22**, 1423 (1969); S. Kim, J. G. Nelson, and R. S. Williams, Phys. Rev. B **31**, 3460 (1985); A. Gupta and R. Sengupta, Phys. Status Solidi B **168**, 455 (1991).
[9] S. Hufner, J. H. Wernick, and K. W. West, Solid State Commun. **10**, 1013 (1972); T. K. Sham, M. L. Perlman, and R. E. Watson, Phys. Rev. B **19**, 539 (1979).
[10] L. S. Hsu, J. D. Denlinger, and J. W. Allen, Mater. Res. Soc. Symp. Proc. **524**, 179 (1998); J. G. Nelson, W. J. Gignac, S. Kim, J. R. Lince, and R. S. Williams, Phys. Rev. B **31**, 3469 (1985).
[11] L. S. Hsu, H. W. Huang, and K. L. Tsang, J. Phys. Chem. Solids **59**, 1205 (1998); T. K. Sham, Solid State Commun. **64**, 1103 (1987).
[12] B. K. Godwal, A. Jayaraman, S. Meenakshi, R. S. Rao, S. K. Sikka, and V. Vijayakumar, Phys. Rev. B **57**, 773 (1998).
[13] B. K. Godwal, S. Meenakshi, P. Modak, R. S. Rao, S. K. Sikka, V. Vijayakumar, E. Bussetto, and A. Lausi, Phys. Rev. B **65**, 140101(R) (2002).
[14] Y. Jeon, B. Qi, F. Lu, and M. Croft, Phys. Rev. B **40**, 1538 (1989); B. Qi, I. Perez, P. H. Ansari, F. Lu, and M. Croft, *ibid.* **36**, 2972 (1987).
[15] W. W. Warren Jr., R. W. Shaw Jr., A. Manth, F. J. Disalvo, A. R. Storm, and J. H. Wernick, Phys. Rev. B **7**, 1247 (1973).
[16] X. Lifshitz, Zh. Eksp. Teor. Fiz. **38**, 1569 (1960) [Sov. Phys. JETP **11**, 1130 (1960)]; L. Dagens, J. Phys. F: Met. Phys. **8**, 2093 (1978).
[17] W. B. Pearson, *Handbook of Lattice Spacing and Structures of Metals and Alloys* (Pergamon, Oxford, 1967), Vol. 2.
[18] V. Vijayakumar, Ph.D. thesis, University of Bombay, 1986.
[19] A. B. Garg, V. Vijayakumar, and B. K. Godwal, Rev. Sci. Instrum. **75**, 2475 (2004).
[20] V. Vjayakumar and S. Meenakshi, Diamond anvil cells for investigation of materials at high pressure BARC Report no. BARC/2000/I/014.
[21] A. P. Hammersley, S. O. Svensson, M. Hanfland, A. N. Fitch, and D. Hausermann, High Press. Res. **14**, 235 (1996).
[22] S. K. Sikka, Phys. Rev. B **38**, 8463 (1988).
[23] P. Blaha, K. Schwarz, G. K. H. Madsen, D. Kvasnicka, and J. Luitz, WIEN2K, An augmented plane wave+local orbitals program for calculating crystal properties, edited by K. Schwarz (TU Wien, Austria, 2001).
[24] J. P. Perdew and Y. Wang, Phys. Rev. B **45**, 13244 (1992).
[25] J. P. Perdew, K. Burke, and M. Ernzerhof, Phys. Rev. Lett. **77**, 3865 (1996).
[26] J. A. Rayne, Phys. Lett. **7**, 114 (1963).
[27] J. M. Leger, J. Haines, and A. Atouf, Phys. Rev. B **51**, 3902 (1995); J. Appl. Crystallogr. **28**, 416 (1995).
[28] J. C. Schon, M. A. C. Wavers, and M. Jensen, J. Phys.: Condens. Matter **15**, 5479 (2003).